

## Numerical simulations for fragmentation dynamics

This article has been downloaded from IOPscience. Please scroll down to see the full text article.

1989 J. Phys. A: Math. Gen. 22 L757

(<http://iopscience.iop.org/0305-4470/22/15/007>)

View [the table of contents for this issue](#), or go to the [journal homepage](#) for more

Download details:

IP Address: 129.252.86.83

The article was downloaded on 01/06/2010 at 06:57

Please note that [terms and conditions apply](#).

## LETTER TO THE EDITOR

# Numerical simulations for fragmentation dynamics

M A F Gomes and G L Vasconcelos

Departamento de Física, Universidade Federal de Pernambuco, 50739 Recife PE, Brazil

Received 23 May 1989

**Abstract.** A geometrical model for the study of fragmentation dynamics is introduced. Detailed statistical analysis of the fragment distribution for percolation clusters, Sierpiński carpets and Menger sponges on square and cubic lattices is given and static and dynamic critical exponents are calculated.

The dynamic behaviour of many phenomena occurring in nature exhibits fragmentation [1-3]. In these cases the system makes a continuous or sudden transition from a connected state to a disconnected state characterised by fragments of diverse sizes. The disconnected or fragmented state may be described if the function  $n(s, t)$  giving the number of fragments of size  $s$  at time  $t$  is known. Fragmentation may occur in processes without variation of mass [1] as well as in growth processes [2] or in consumption processes [3].

In this letter we present results of extensive numerical simulations of fragmentation dynamics in porous (fractal) systems on square and cubic lattices. Our fragmentation model simulates the attack of a system by a kind of corrosive rain. The units (drops) that form this rain may be considered as molecules of a chemical reagent in some corrosion process or, alternately, a mechanical stress acting randomly on a system or again a combination of both chemical and mechanical agents in a stress-assisted corrosion. In addition, the drops may be a pathogenic element/plague acting on a tissue/plantation. To allow numerical simulations on large lattices and to perform a detailed statistical analysis of the results, we avoid intricacies and choose a fragmentation algorithm governed by the following simple laws.

(A) If a drop hits a site  $i$  of the system whose number  $q(i)$  of nearest neighbours satisfies  $q(i) < 2d$ , that point is eliminated (the system is embedded in a  $d$ -dimensional square lattice and  $2d$  is the lattice coordination number). Using the analogy with a chemical attack, we consider that a drop  $x$  combines irreversibly with the site  $i$  giving a reaction product  $xi$ . These products are deleted in the course of the simulation since they are a different species.

(B) A point  $i$  of the system survives the attack if  $q(i) = 2d$ .

According to these rules, points weakly connected to the system (in the sense  $q < 2d$ ) are always vulnerable to the attack, while points with maximal coordination ( $q = 2d$ ) are immune to the attack. Evidently, the neighbourhood of the site  $i$  changes with the time and in a later stage this site will be consumed. When we apply this algorithm to a system embedded in a two-dimensional lattice, the rain is assumed to fall along the third dimension, and when we apply it to a system embedded in a cubic lattice (a three-dimensional hyperplane), the rain is falling along a fourth dimension. The following observations are pertinent. As in a true rain, it is considered possible

that a consumed site may be visited many times by raindrops till the end of the simulation. Thus, we have a direct correspondence between the physical time  $T$  and the computational time  $t = \text{total number of raindrops that fell on the system} = F \times T$ , where  $F$  is the number of raindrops falling per unit time. The equation of motion of this fragmentation process is  $(dM/dt) = -c \times m$ , where  $M$  is the mass of the system,  $c$  is a constant (dependent on parameters or macroscopic variables relevant to a particular situation) and the active mass or perimeter  $m$  is the set  $\{i \in \text{system} | q(i) < 2d\}$ .

The porous systems studied in this letter are percolation clusters (PC) in  $d = 2, 3$  at the respective percolation thresholds [4], Sierpiński carpets (SC) in  $d = 2$  and Menger sponges (MS) in  $d = 3$  [5, p 144]. The fractal dimensions for these systems are, respectively, 1.896, 2.5,  $(\ln 8 / \ln 3) \approx 1.8928$  and  $(\ln 20 / \ln 3) \approx 2.7268$ . The lattice sizes were  $L = 2001$  ( $d = 2$ ) and  $L = 101$  ( $d = 3$ ) for PC,  $L = 2187$  (corresponding to an initial mass  $M_0 = 8^7 = 2\,097\,152$ ) for SC and  $L = 243$  ( $M_0 = 20^5 = 3\,200\,000$ ) for MS. We have examined the fragment distribution function  $n(s, t)$  as well as the time dependence of the mean fragment size,  $\langle s \rangle$ , on the total number of fragments,  $N(t)$ , and the diversity of the fragments,  $\Delta(t)$ , which is the number of different fragment sizes present at time  $t$ . The following scaling relations were observed before the maximum in  $N(t)$  was reached:  $N(t) \sim t^\Phi$  (figures 1 and 2);  $n(s, t) \sim t^W$ , for small values of  $s$  (figures 3 and 4) and  $\langle s \rangle \sim t^{-Z}$  (figure 5). Furthermore,  $n(s, t) \sim s^{-\Theta}$  (figure 6) for  $t$  not too far from the time of maximal fragmentation. Figures 1–6 refer to results averaged on ten similar experiments. The critical exponents  $\Phi, W, Z$  and  $\Theta$  are shown in table 1. For comparison we add in this table the exponents for fragmentation of two-dimensional Euclidean rings [3]. An examination of table 1 shows that the three dynamic exponents  $\Phi, W$  and  $Z$  and the static exponent  $\Theta$  for PC and SC/MS are weakly dependent on  $d$ . The relative uncertainties on these exponents are  $(\Delta\Phi/\Phi) = 0.1$ ,  $(\Delta W/W) = (\Delta Z/Z) = 0.2$  and  $(\Delta\Theta/\Theta) = 0.15$ . The exponents  $\Phi$  and  $\Theta$  for rings are close to the values observed for PC. The possibility that  $\Phi \approx W \approx 1$  also for rings is not excluded since the simulations with these systems were made on small lattices ( $L \approx 100$ ). However, the critical exponents for SC and MS are significantly different from those obtained for PC and

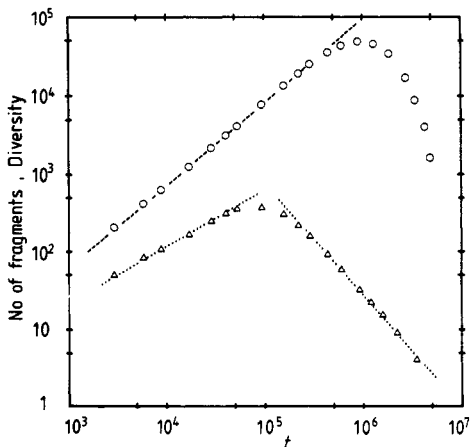


**Figure 1.** The total number of fragments ( $\circ$ ) and the diversity ( $\Delta$ ) as a function of time for two-dimensional percolation clusters on a square lattice with edge  $L = 2001$ . The dashed line corresponds to a slope of 1.06 (see text for more details).

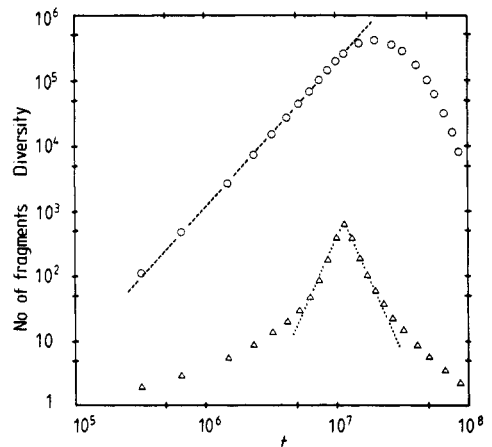


**Figure 2.** The same as in figure 1 but for Menger sponges on cubic lattices ( $L = 243$ ). Initial mass of the sponges:  $M_0 = 3\,200\,000$ . The slope of the dashed line is 2.24.

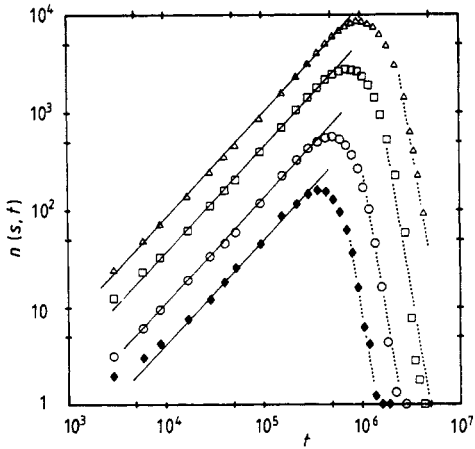


**Figure 3.** Time dependence of the distribution function  $n(s, t)$  for fragment sizes  $s = 2$  ( $\Delta$ ),  $4$  ( $\square$ ),  $10$  ( $\circ$ ) and  $20$  ( $\blacklozenge$ ), calculated from the same simulations as in figure 1. Full lines have the slope 1.07.

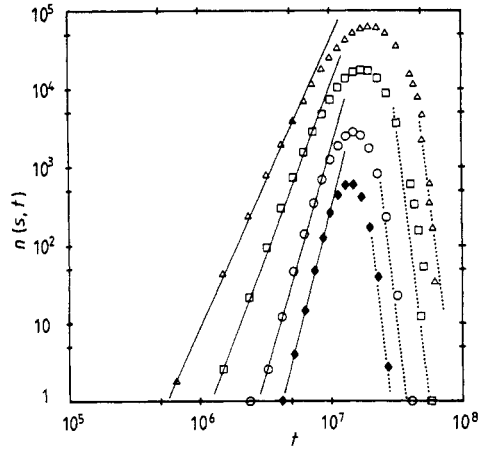


**Figure 4.** The same as in figure 3 but for Menger sponges in  $d = 3$ . Each full line in this case has a different slope (compare with figure 3 and see text for details).

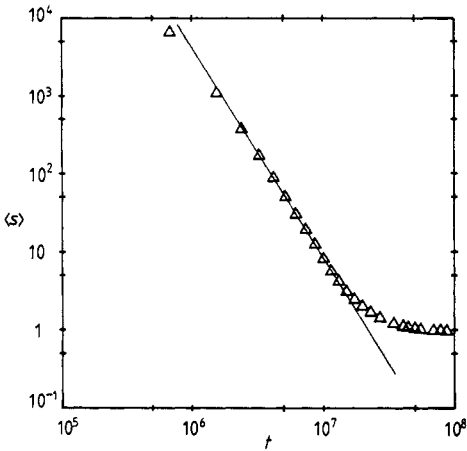


**Figure 5.** The average size  $\langle s \rangle$  of the fragments as a function of the time for the clusters of figure 2. The straight line corresponds to an asymptotic slope of  $-2.69$ .

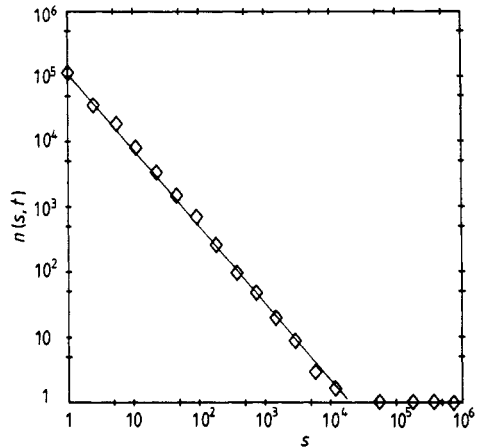


**Figure 6.** The size dependence of the distribution function  $n(s, t)$  at the time of maximal fragmentation for Menger sponges ( $d = 3$ ). The straight line has a slope of  $-1.16$ .

rings. The large differences between the exponents for PC and SC in  $d = 2$  (systems with almost the same fractal dimension) show the importance of the topological properties of the system in the fragmentation process. Another remarkable fact is that the exponent  $W$  for SC and MS depends on  $s$ , contrary to what is observed with the other systems. This fact is illustrated in figures 3 and 4. The dependence of  $W$  on  $s$ , for  $1 \leq s \leq 20$  is  $W = 2.27 \times s^{0.27}$  for SC and  $W = 3.1 \times s^{0.26}$  for MS. The results of table 1 indicate that the total mass  $M(t) = N(t) \times \langle s \rangle$  decreases in the scaling region as  $M \sim t^A$ , with  $A = \Phi - Z$  assuming values between  $-0.2$  and  $-0.45$ . Figures 1 and 2 show the qualitative difference between the behaviours of the diversity for PC and

**Table 1.** The exponents appearing in the scaling relations  $N \sim t^\Phi$ ,  $n(s, t) \sim t^W$ ,  $\langle s \rangle \sim t^{-Z}$ , and  $n(s, t) \sim s^{-\Theta}$  (at the time of maximal fragmentation). These numbers are average values obtained from a best fit using ten similar experiments. See text for more details.

System	$\Phi$	$W$	$Z$	$\Theta$
PC ( $d = 2$ )	1.06	1.07	1.23	0.45
PC ( $d = 3$ )	0.981	1.02	1.15	0.52
SC ( $d = 2$ )	2.33	2.27-5.37	2.54	0.926
MS ( $d = 3$ )	2.24	3.1-6.6	2.69	1.16
Rings ( $d = 2$ )	$1.2 \pm 0.3$	$1.8 \pm 0.4$	$1.5 \pm 0.4$	$0.6 \pm 0.1$

MS(SC). Although both systems in these figures have  $M_0$  (and  $\Delta$  maximum) of the same order, the increase of  $\Delta(t)$  near the maximum is much faster for MS (SC) than for PC. The behaviour of  $\Delta(t)$  on the left (right) side of  $\Delta$  maximum (dotted lines in figures 1 and 2) may be described by a power law of  $t$  with the exponents 0.73 (-1.43), 0.67 (-1.36); 4.19 (-3.36) and 4.53 (-4.61) for PC in  $d = 2, 3$ ; SC and MS, respectively. Again, there are no appreciable differences between the corresponding exponents for  $d = 2$  and  $d = 3$ . On the other hand, the fragment-size distribution function  $n(s, t)$  may be described to the right of their maximum by a power law of  $t$  (dotted lines in figures 3 and 4) with an exponent  $W^*$  which seems independent of  $s$ , for small  $s$ . The values of this exponent are approximately -6, -10; -10 and -14 for PC in  $d = 2, 3$ ; SC and MS, respectively. We note, however, that this scaling occurs in a much more restricted time interval than that observed to the left of the extremum of  $n(s, t)$ . Furthermore, in the scaling region governed by  $W^*$ ,  $\langle s \rangle$  does not present power-law scaling in  $t$ . The dependence on the lattice size  $L$  of the exponents of table 1 was also investigated:  $\Phi$ ,  $W$ ,  $Z$  and  $\Theta$ (PC) stabilised around the reported values more rapidly than  $\Theta$ (SC) and  $\Theta$ (MS). The average percentage difference between the exponents of table 1 for  $d = 2$  ( $L > 2000$ ) and the corresponding exponents for  $L \approx 300$  is 21%.

The maximum in the distribution function  $n(s, t)$  occurs at a time  $t[s]$  dependent on the fragment size  $s$  (figures 3 and 4). We have found that  $\max - n(s, t) \sim s^{-\Psi}$  at  $t = t[s]$  and  $t[s] \sim s^{-\Omega}$ . The exponents  $\Psi$  and  $\Omega$  are given in table 2. Furthermore, the maximal values observed for  $N(t)$  and  $\Delta(t)$  (figures 1 and 2) are clearly dependent on the initial mass  $M_0$ . Simulations realised with PC and SC in  $d = 2$  with masses varying by a factor near 200 showed that  $\max - N \sim M_0^K$  and  $\max - \Delta \sim M_0^\Lambda$ , with  $K$  and  $\Lambda$  given in table 3. The maxima in  $N$  and  $\Delta$  occur at times  $T[N]$  and  $T[\Delta]$ , respectively. These times also scale with the initial mass  $M_0$  as  $T[N] \sim M_0^\Gamma$  and  $T[\Delta] \sim M_0^\Xi$ , and these exponents are also shown in table 3. Recent estimates of the exponents  $K$  and  $\Gamma$  using renormalisation group calculations on small cells [6] are in agreement with the results of table 3.

**Table 2.** The exponents  $\Psi$  and  $\Omega$  from the scaling relations  $\max - n(s, t) \sim s^{-\Psi}$  at  $t[s] \sim s^{-\Omega}$  (see text).

	PC ( $d = 2$ )	PC ( $d = 3$ )	SC ( $d = 2$ )	MS ( $d = 3$ )
$\Psi$	1.67	1.79	1.81	2.04
$\Omega$	0.41	0.55	0.215	0.165

**Table 3.** The exponents  $K$ ,  $\Lambda$ ,  $\Gamma$  and  $\Xi$  which appear in the scaling relations  $\max - N \sim M_0^K$ ,  $\max - \Delta \sim M_0^\Lambda$ ,  $T[N] \sim M_0^\Gamma$  and  $T[\Delta] \sim M_0^\Xi$  (details in text).

	PC ( $d = 2$ )	SC ( $d = 2$ )
$K$	0.646	1.01
$\Lambda$	0.313	0.498
$\Gamma$	0.67	1.04
$\Xi$	0.53	0.997

Another quantity of interest is the integrated fragment distribution,  $N(>s)$ , which gives the number of fragments with size greater than  $s$  [7]. This function has been studied for PC and SC in  $d = 2$  in the neighbourhood of the time of maximal fragmentation. In these cases  $N(>s) \sim s^{-B}$ , with  $B$  assuming the values  $0.53 \pm 0.03$  for PC, and  $0.65 \pm 0.04$  for SC. The power-law dependence of  $N(>s)$  on  $s$  implies the absence of a length scale on a large interval of  $s$  and is characteristic of a fractal distribution. In fact, these numbers indicate that the fragments in  $d = 2$  at the time of maximal fragmentation (or close to it) are distributed on fractal sets of dimension  $2B$  [5, ch 13]; thus we have the fractal dimensions  $1.06 \pm 0.06$  for PC, and  $1.3 \pm 0.08$  for SC. We note in passing that the corresponding value of  $B$  for Euclidean rings is  $0.55 \pm 0.04$  [3]. Thus, these static exponents  $B$  are close to the exponents  $\Theta$  given in table I.

The results reported in this letter for PC are in agreement with a dynamic scaling proposed by Vicsek and Family for cluster-cluster aggregation [8]. For our fragmentation model this scaling is  $n(s, t) = t^W s^{-\Theta} \phi(s/t^Z)$ , with  $\phi(x)$  satisfying  $\phi(x) = \text{constant}$ , for  $x \ll 1$ , and  $\phi(x) \ll 1$ , for  $x \gg 1$ . From this scaling it follows that the exponent  $\Phi$  introduced in the third paragraph is given by  $\Phi = W - Z(1 - \Theta)$ .

We thank A L T Azevedo and S Meira for discussions in the early stages of this work and N Peddersen for technical assistance. One of us (MAFG) acknowledges the hospitality at the Dipartimento di Fisica of Università di Padova and in particular A L Stella for valuable discussions and comments on the manuscript. Discussions with A Maritan are gratefully acknowledged.

This work was supported in part by FINEP and CNPq (Brazilian government agencies).

## References

- [1] Grady D E and Kipp M E 1985 *J. Appl. Phys.* **58** 1210-22
- [2] Williams T and Bjerkness R 1972 *Nature* **236** 19-21
- [3] Gomes M A F and Vasconcelos G L 1988 *Preprint* (presented at the Second Workshop on Scaling, Fractals and Nonlinear Variability in Geophysics (Paris 1988))
- [4] Stauffer D 1985 *Introduction to Percolation Theory* (London: Taylor and Francis)
- [5] Mandelbrot B B 1983 *The Fractal Geometry of Nature* (San Francisco: Freeman)
- [6] Gomes M A F, Maritan A, Stella A L and Vasconcelos G L 1989 unpublished
- [7] Englman R, Rivier N and Jaeger Z 1987 *Phil. Mag. B* **56** 751-69
- [8] Vicsek T and Family F 1984 *Phys. Rev. Lett.* **52** 1669-72